Title

Libman-Sacks Endocarditis: Detection, Characterization, and Clinical Correlates by Three-Dimensional Transesophageal Echocardiography

Journal

Journal of the American Society of Echocardiography, 28(7)

ISSN

0894-7317

Authors

Roldan, Carlos A
Tolstrup, Kirsten
Macias, Leonardo
et al.

Publication Date

2015-07-01

DOI

10.1016/j.echo.2015.02.011

Peer reviewed

HHS Public Access

Author manuscript

J Am Soc Echocardiogr. Author manuscript; available in PMC 2016 July 01.

Published in final edited form as:

J Am Soc Echocardiogr. 2015 July ; 28(7): 770–779. doi:10.1016/j.echo.2015.02.011.

LIBMAN-SACKS ENDOCARDITIS: DETECTION, CHARACTERIZATION, AND CLINICAL CORRELATES BY THREE-DIMENSIONAL TRANSESOPHAGEAL ECHOCARDIOGRAPHY

Carlos A. Roldan, M.D., **Kirsten Tolstrup, M.D.**, **Leonardo Macias, M.D.**, **Clifford R. Qualls, Ph.D.**, **Diana Maynard, RCS**, **Gerald Charlton, M.D.**, and **Wilmer L. Sibbitt Jr, M.D.**

Department of Medicine and Divisions of Cardiology and Rheumatology University of New Mexico School of Medicine and New Mexico VA Health Care Center, Albuquerque, New Mexico, USA.

Abstract

Background—Libman-Sacks endocarditis, characterized by Libman-Sacks vegetations, is common in patients with systemic lupus erythematosus (SLE), and is commonly complicated with embolic cerebrovascular disease. Thus, accurate detection of Libman-Sacks vegetations may lead to early therapy and prevention of their associated complications. Although two-dimensional transesophageal echocardiography (2D-TEE) has high diagnostic value for detection of Libman-Sacks vegetations, three-dimensional TEE (3D-TEE) may allow improved detection, characterization, and clinical correlations of Libman-Sacks vegetations.

Methods—29 SLE patients (27 women, age 34±12 years) prospectively underwent 40 paired 3D-TEE and 2D-TEE studies and assessment of cerebrovascular disease manifested as acute clinical neurologic syndromes, neurocognitive dysfunction, or focal brain injury on MRI. Initial and repeat studies in patients were intermixed in a blinded manner with paired studies from healthy controls, de-identified, coded, and independently interpreted by experienced observers unaware of patients' clinical and imaging data.

Results—3D-TEE as compared to 2D-TEE studies were more often positive for mitral or aortic valve vegetations, detected more vegetations per study, and determined larger size of vegetations (all $p \leq 0.03$). Also, 3D-TEE detected more vegetations on the anterior mitral leaflet, anterolateral and posteromedial scallops, and ventricular side or both atrial and ventricular sides of the leaflets (all $p < 0.05$). In addition, 3D-TEE detected more vegetations on the aortic valve left and non-coronary cusps, coronary cusps' tip and margins, and aortic side or both aortic and ventricular sides of the cusps (all $p \leq 0.01$). Furthermore, 3D-TEE detected more often associated mitral or aortic valves' commissural fusion ($p = 0.002$). Finally, 3D-TEE detected more vegetations in patients with cerebrovascular disease ($p = 0.01$).

Conclusion—3D-TEE provides clinically relevant additive information that complements 2D-TEE for the detection, characterization, and association with cerebrovascular disease of Libman-Sacks endocarditis.

Address for Correspondence: Carlos A. Roldan, M.D., F.A.C.C., F.A.S.E., Professor of Medicine, University of New Mexico School of Medicine, Cardiology Division 5-ACC, 1 University of New Mexico, MSC 50-5550, Albuquerque New Mexico 87131-0005, Phone: 505-272-6020, Fax 505-272-4362, croldan@salud.unm.edu.

Keywords

Libman-Sacks endocarditis; Libman-Sacks vegetations; Systemic lupus erythematosus; Valvular heart disease; Three-dimensional transesophageal echocardiography; Two-dimensional transesophageal echocardiography; Cerebrovascular disease

INTRODUCTION

Libman-Sacks endocarditis, best characterized by Libman-Sacks vegetations, is common in systemic lupus erythematosus (SLE). Libman-Sacks vegetations are sterile abnormal growths of tissue around the heart valves with an autoimmune-mediated inflammatory and thrombotic pathogenesis (1–4). Libman-Sacks vegetations can be complicated with embolic cerebrovascular disease, peripheral arterial embolism, severe valve regurgitation, superimposed infective endocarditis, need for high risk valve surgery, and increased mortality (5–11). Therefore, accurate detection of Libman-Sacks endocarditis may lead to early therapy and prevention of the development or progression of its associated complications. Multiplane two-dimensional (2-D) transesophageal echocardiography (TEE) has high diagnostic value for detection of Libman-Sacks endocarditis (5,6,8,12). Three-dimensional TEE (3D-TEE) has emerged as an important complementary technique to 2D-TEE for detection and characterization of infective vegetations and valve tumors (13–16). However, no previous study has been reported on the diagnostic value and clinical relevance of 3D-TEE in Libman-Sacks endocarditis. Therefore, this 3-year duration study was prospectively designed and conducted to determine the value of 3D-TEE as compared to 2D-TEE for the detection, characterization, and association with cerebrovascular disease of Libman-Sacks vegetations.

METHODS

Study Population

This study was part of a 6-year duration (December 2006 to December 2012) research protocol approved by the National Institutes of Health and Institutional Review Board for the study of cardiovascular and cerebrovascular disease in patients with SLE. The results of that study in 102 subjects (76 SLE patients and 26 healthy controls) using 2D-TEE have been published (8). All participants provided informed consent.

From February 2010 (time when 3D-TEE became available at our institution) to December 2012 (end of study funding and authorized enrollment), 29 SLE patients [27 women, age 34±12 years (range,18–55)] prospectively underwent clinical and laboratory evaluations, brain MRI, neurocognitive assessment, and 40 paired 3D-TEE and 2D-TEE studies (11 studies were repeated to reassess cardiac and brain disease after anti-inflammatory and/or antithrombotic therapy after patients' first or during recurrent neurologic events). The 40 paired TEE studies constitute the basis for this study.

Patients with suspected heart and brain disease unrelated to SLE including any febrile illness and infective endocarditis were excluded from participation in the study.

Clinical, laboratory, brain MRI, and TEE initial and repeat paired studies in patients were intermixed in a blinded manner with paired studies from healthy controls, were de-identified, coded, and independently interpreted by experienced observers unaware of patients' clinical and imaging data.

Clinical, brain MRI, and laboratory evaluations—On enrollment, patients were prospectively assessed for the presence of 1) acute or recent focal and non-focal neurologic syndromes of stroke, transient ischemic attack (TIA), confusional state, cognitive dysfunction, or seizures (8,17); 2) focal brain injury on MRI defined as old or recent cerebral infarcts or periventricular or deep white matter abnormalities (8,18); and 3) global neurocognitive dysfunction defined as ≥1.5 standard deviations bellow the mean of healthy controls (8,19). Patients were also characterized with regard to SLE duration, activity, damage, standard serology, autoantibodies including antiphospholipid antibodies, and anti-inflammatory and anti-thrombotic therapy (Table 1).

Transesophageal echocardiography—Participants underwent concurrent, complete 3D-TEE and 2D-TEE with IE-33 Philips systems (Andover Massachusetts, USA) using a 7 MHz 3D matrix-array transducer. Images were digitally acquired for off-line reconstruction (for 3D-TEE images) and interpretation.

Using 2D-TEE and from basal to mid esophageal levels, the mitral and aortic valves were imaged in multiple planes at a depth of 4–8 cm with a narrow sector scan to improve image resolution (5,8,12,20).

Using 3D-TEE and from basal to mid-esophageal levels, 0–120 degrees views of the mitral valve and 30–60 degrees short axis and 110–130 degrees long axis views of the aortic valve were acquired. To achieve the highest spatial and temporal resolution, electrocardiographically triggered multiple-beat (4 beats) high density full volume images with the narrowest possible sector scan were obtained during breath holding (expiration). 3D-TEE full-volume data sets were acquired with gain and compression settings of ≥50 units and then cropped and multiplane transected to obtain en-face atrial and left ventricular views of the mitral valve and aortic root and left ventricular outflow tract views of the aortic valve (20,21).

2D-TEE and 3D-TEE images were acquired during the same examination and both types of images were collected by the same examiner using the same TEE probe. Also, 2D-TEE images were acquired in a systematic order using single or infrequently x-plane tomographic planes. In addition, volumetric images were obtained in a systematic manner independently of identifying or not valve pathology on single tomographic planes. Furthermore, for best quality matching of 2D and 3D-TEE images, 3D-TEE volumetric images were obtained immediately after the best corresponding 2D images.

To reduce interpretation bias toward 3D-TEE, the following steps were taken: 1) No live 3D images were obtained or recorded during the performance of TEE studies. 2) All de-identified 2D-TEE studies were first interpreted by one experienced observer (CAR). In 22 randomly selected 2D-TEE studies, inter-observer agreement (CAR and GAC) for detection

of vegetations of the mitral, aortic, and either valve were 82% (Kappa 0.61), 96% (Kappa 0.91), and 91% (Kappa 0.80), respectively. 3) At a later time and in order to preserve the highest image resolution, 3D-TEE studies of the mitral and aortic valves were identified by analyzing the volumetric datasets using multiplanar reconstruction in the ultrasound imaging systems by an experienced observer (DM) who was not an interpreter of TEE studies. These images were usually added at the end of the study. Finally, 4) 3D-TEE studies were independently interpreted by 2 experienced observers (CAR and KT) unaware of earlier 2D-TEE interpretations. For all 3D-TEE studies, inter-observer agreement (CAR and KT) for detection of vegetations of the mitral, aortic, and either valve were 89% (Kappa 0.78), 97% (kappa 0.92), and 96% (Kappa 0.92), respectively.

Criteria for 3D-TEE and 2D-TEE Interpretation—*Libman-Sacks vegetations* by either technique were defined as abnormal localized, protruding, and sessile echodensities of >3 mm in diameter with well-defined borders either as part of or adjacent to valve leaflets, annulus, subvalvular apparatus, or endocardial surfaces (1–8,12,13). The cutoff of >3 mm in diameter was adopted to prevent misinterpretation of Lambl's excrescences as vegetations. Lambl's excrescences are thin (usually ≤2 mm in width, rarely up to 3 mm), elongated (usually >5 mm in length), independently hypermobile, and homogeneously echoreflectant structures located at the coaptation point and atrial side of the mitral valve and ventricular side of the aortic valve (22). By both techniques, location of the mitral valve vegetations with regard to anterior or posterior leaflets; basal, mid, or distal portions of the leaflets; corresponding scallops [anterolateral (A1, P1), middle (A2, P2), or posteromedial (A3, P3)]; and atrial or ventricular side of the leaflets was determined. Location of the aortic valve vegetations with regard to left, right, or non-coronary cusps; tip, body, or margin of the cusps; and ventricular or aortic side of the cusps was also determined.

Using multiplane 2D-TEE, the maximum diameter and area of vegetations were measured. With 3D-TEE, the maximum diameter and area of vegetations were measured from the anteroposterior, superoinferior, and mediolateral dimensions. These 3D-TEE measurements were performed off-line using Q lab and multiplanar reconstruction mode. For both techniques and using electronic calipers, 3 measurements during 3 different cardiac cycles were performed and the maximum diameters and areas were analyzed.

The presence and severity of associated mitral valve anterolateral or posteromedial commissural fusion was assessed from the atrial view and defined as mild, moderate, or severe when involved ≤one third, up to two thirds, or the entire corresponding commissural scallops, respectively. Aortic valve commissural fusion was assessed from the aortic root view and defined as mild, moderate, or severe when the corresponding cusps were fused ≤one third, up to two thirds, or extended to the cusps' central coaptation point, respectively.

Finally, the detection of valve vegetations by 3D-TEE and 2D-TEE in relation to acute clinical neurologic syndromes, focal brain injury on MRI, neurocognitive dysfunction, or the combination of these 3 outcomes was determined.

Statistical analysis

Descriptive statistics were frequencies (%) and mean ± SD. Paired comparison of the number of 3D-TEE versus 2D-TEE studies with vegetations and the frequency of vegetations by either technique in relation to cerebrovascular disease were performed by McNemar's test. The individual mean counts of vegetations per study are reported as Poisson means. These mean counts with regard to locations [distal versus mid or proximal leaflet and middle (A2 or P2) versus anterolateral or posteromedial (A1, P1 or A3, P3) scallops for the mitral valve leaflets and left, non, or right coronary cusps and cusp tip, body, or margin for the aortic valve cusps] as repeated factors were done by Poisson regression [PROC GENMOD in SAS]. The comparisons of diameters and areas of vegetations between 3D-TEE and 2D-TEE were done by paired t-tests. Two tailed p-values ≤0.05 were considered significant. All statistical analyses were performed using SAS 9.3.

RESULTS

Clinical and laboratory evaluations

Among the 40 patients with SLE who underwent TEE studies, a total of 34 (85%) had one or more manifestation of cerebrovascular involvement: 23 (58%) patients had acute neurologic syndromes, 25 (63%) had focal brain injury on MRI, and 27 (68%) had neurocognitive dysfunction. As shown in Table 1, SLE patients were young, had a mean disease duration of 6.2 years, had high inflammatory markers, nearly 60% had positive anti-phospholipid antibodies, the majority (55%) were receiving prednisone for nearly 5 years, 41% were on non-steroidal immunosuppressive therapy, and 38% were on antiplatelet or anticoagulant therapy.

Detection and characterization of Libman-Sacks vegetations by 3D-TEE and 2D-TEE

As shown in Table 2, 3D-TEE as compared to 2D-TEE studies were more often positive for mitral valve, aortic, and either valve vegetations (all $p<0.05$); detected higher number of aortic valve vegetations and either valve vegetations (Poisson regression, both $p \leq 0.01$) with a trend for mitral valve vegetations ($p=0.09$); and determined larger diameter and area of mitral valve vegetations (both $p<0.05$) and larger maximum diameter of aortic valve vegetations ($p=0.005$).

Also, as shown in Table 3, 3D-TEE as compared with 2D-TEE improved localization of vegetations. 3D-TEE detected more vegetations on the anterior mitral leaflet, anterolateral (A1, P1) and posteromedial (A3, P3) mitral scallops, and on the ventricular side or both ventricular and atrial side (vegetations probably extending into both sides) of the leaflets (all $p<0.05$) (Figures 1–3 **with video clips**). In addition, 3D-TEE detected a higher number of vegetations on the anterior or posterior mitral leaflets with an oval, tubular or roll-like, coalescent, or clustered shape affecting 2 or 3 contiguous scallops ($p=0.03$) (Figures 1–3). The location of mitral valve vegetations on the ventricular side or on both sides of the leaflets and vegetations affecting 2 or more contiguous scallops were originally described by Libman & Sacks (1). Furthermore, 3D-TEE detected more aortic valve vegetations on the left and non-coronary cusps, on the coronary cusps' tip and margins, and on both aortic and

ventricular side (vegetations extending into both sides) of the cusps (all p≤0.009) (Figures 4 & 5 **with video clips**).

It is worth emphasizing that, compared with 2D-TEE, the use of 3D-TEE provided additional information about the aortic valve more often than for the mitral valve. As shown in Tables 2 & 3, while the number of studies demonstrating vegetations, the number of vegetations identified, and the different locations of vegetations were higher using 3D-TEE as compared with 2D-TEE, these differences were generally most striking for the aortic valve. This is likely explained by the superior visualization of the bodies of the aortic cusps using 3D-TEE.

In addition, as shown in Table 4, 3D-TEE detected more often associated commissural fusion of the mitral leaflets or aortic cusps (p=0.002), which was characterized as mild in 11 of 12 (93%) cases.

Finally, as shown in Table 5, 3D-TEE as compared to 2D-TEE detected more vegetations in patients with acute neurologic syndromes, stroke/TIA, focal brain injury on MRI, neurocognitive dysfunction, or any cerebrovascular disease (overall p=0.01).

DISCUSSION

Major Findings

In this prospectively conducted study, 3D-TEE as compared to 2D-TEE studies were more often positive for Libman-Sacks vegetations, detected higher number of vegetations, and determined larger size of vegetations; defined better the location, extent, shape, and appearance of vegetations; detected more often associated leaflets' or cusps' commissural fusion; and of most importance, detected higher frequency of vegetations in patients with cerebrovascular disease. Therefore, the study findings are of clinical relevance and add to previous studies in general populations and 5 isolated case reports of Libman-Sacks endocarditis on the complementary value of 3D-TEE to 2D-TTE or 2D-TEE for the detection, characterization, and differentiation of non-infective and infective vegetations, valve tumors, thrombus, and nodular calcifications (13–16,23–28,). Also, 3D-TEE may have additive complementary value to 2D-TEE in the diagnosis of embolic cerebrovascular disease in SLE.

Clinical Implications

Libman-Sacks vegetations are strong independent risk or pathogenic factors for stroke or TIA, focal brain lesions on MRI, or cognitive disability and can be further complicated with acute or chronic severe valve dysfunction, superimposed infective endocarditis, need for high risk valve surgery, and ultimately with death (1,5–11,26–28). This study demonstrates that 3D-TEE provides clinically relevant additive information that complements 2D-TEE for the detection and characterization of Libman-Sacks vegetations and may also provide an improved assessment of cardioembolic cerebrovascular disease in SLE patients. Thus, early and accurate detection of Libman-Sacks vegetations using 3D-TEE may lead to early anti-inflammatory and antithrombotic therapy and prevention of the development or progression of their associated complications. Due to the semi-invasive nature of TEE, SLE patients

should be carefully selected for undergoing TEE with the highest diagnostic yield. We consider appropriate to perform 3D-TEE in SLE patients with 1) acute, recent, or recurrent stroke or TIA; 2) acute, recent, or recurrent confusional state, cognitive dysfunction, or seizures and focal brain lesions on MRI (8); 3) moderate or worse valve regurgitation on TTE; or 4) suspected superimposed infective endocarditis. In this study, 3D-TEE distinctively characterized Libman-Sacks vegetations as sessile, oval or tubular or coalescent in shape, nodular or protruberant, heterogeneously or homogeneously echoreflectant, predominantly located on the leaflets' coaptation point but frequently extending through the leaflets into the opposite side, and uncommonly associated with significant valve regurgitation. These echocardiographic characteristics and in particular their sessile mobility may be explained by the histopathology described by Libman & Sacks and others (1–4) as follows: a) Libman-Sacks endocarditis involves the entire surface and thickness of the leaflets (atrial and ventricular side of mitral leaflets and aortic and ventricular side of aortic cusps); b) Libman-Sacks vegetations are located predominantly along the leaflets' coaptation point, but frequently extend into the mid and basal portions and into the opposite side through the entire thickness of the leaflets and are therefore always associated with leaflets' thickening; c) Libman-Sacks vegetations are verrucous or granular in appearance and usually coalescent or in clusters; d) Libman-Sacks vegetations are more commonly "mixed" (vegetations with intermixed areas of activity and healing with superimposed platelet thrombi with variable degrees of hyalinization and endothelialization) and/or "healed" type (vegetations with fibroblastic proliferation, central fibrosis, neovascularization, minimal to no inflammation, and peripherally an organized or hyalinized thrombus with partial or full endothelialization or no thrombus at all), and less often "active" vegetations (those with central myxoid degeneration, fibrinoid necrosis, and hemorrhages surrounded by predominant polymorphonuclear cell inflammation and peripherally by platelet thrombi); and therefore, e) Libman-Sacks vegetations have a broad, deep, and firm attachment to the leaflets. These histopathologic characteristics may be related to the highly variable SLE activity (flares alternating with remissions) and its usual standard anti-inflammatory and/or anti-thrombotic therapy including cloroquine or hydroxycloroquine (both with anti-inflammatory and antithrombotic effects, 69% of patients were on this therapy in this study), corticosteroids (55%), non-steroidal immunosuppressive therapy (41%), and antiplatelets or anticoagulants (38% in this study). All these factors may also explain the uncommon significant valve dysfunction (regurgitation or stenosis) and absence of valve perforations in patients with Libman-Sacks endocarditis in contrast to the frequent finding of moderate or severe valve regurgitation and valve perforations in patients with infective endocarditis. The described echocardiographic features should help to differentiate Libman-Sacks vegetations from the independently highly mobile, narrow base attachment, and elongated infective vegetations, Lambl's excrescences, and papillary fibroelastomas (13–16,22–29). However, the presumed echocardiographic diagnosis of non-infective vegetations requires integration of clinical and laboratory data and in some cases of bacteriologic studies. Finally, a larger cross-sectional and longitudinal study is needed to determine the diagnostic and prognostic value of 3D-TEE for detecting Libman-Sacks endocarditis and its associated complications and assessing their response to anti-inflammatory and antithrombotic therapy.

Study limitations

Although the study population was relatively small, this is in fact a larger 3D-TEE study as compared to previous studies of non-infective and infective valve masses consisting of <20 patients (13–16,23). Lack of a 1 to 1 matched control group may have led to interpretation bias for detection of Libman-Sacks vegetations by both 3D-TEE and 2D-TEE. However, the 40 paired TEE studies were de-identified, codified, and independently interpreted by observers unaware of subjects' clinical data. Also, interpreters were aware that these 40 studies were part of the parent study where images of 76 patients and 26 healthy controls were randomly intermixed at a variable ratio for suppression of interpretation bias (8). In fact, 4 paired (3D-TEE and 2D-TEE) de-identified studies of controls were intermixed with 40 paired studies of patients. No vegetations were detected by either technique in those 4 controls. Due to low surgical or mortality rate (3/29=10%) of the study group, 3D-TEE findings lack surgical or pathologic confirmation (except for 1 patient, Figure 1) for assessment of its diagnostic accuracy. However, 3D-TEE findings of infective and non-infective valve masses correlate highly with those of surgical or pathologic findings in non-SLE populations (13–16,23). The study did not assess the diagnostic value of 3D-TEE for right sided vegetations because they are rare (3.4% in this study) and their visualization by 2D-TEE and 3D-TEE may not be superior to that of 2D-TTE and 3D-TTE (5,8,24). The study did not assess extensively valve regurgitation because ≥mild mitral or aortic regurgitation was demonstrated in 7 patients (18%) by 3D-TEE and in 8 patients (20%) by 2D-TEE and ≥moderate valve regurgitation occurred only in 3 patients (7.5%) by both techniques (5,8,20,21,30–32). Also, valve thickening was not assessed since the temporal and spatial resolution of 3D-TEE for assessment of valve thickening may be limited (33).

Conclusion

This study demonstrates that 3D-TEE provides clinically relevant additive information that complements 2D-TEE for the detection, characterization, and association with cerebrovascular disease of Libman-Sacks endocarditis.

Supplementary Material

Refer to Web version on PubMed Central for supplementary material.

ACKNOWLEDGEMENT

This research was funded by the grant RO1-HL04722-01-A6 by the National Institutes of Health/National Heart Lung and Blood Institute and in part by the grant 8UL1-TR000041 by the National Center for Research Resources.

Also, especial thanks to Heather Jarrell, M.D., Assistant Professor of Pathology, for the histopathologic illustrations and expert description of Libman-Sacks vegetations.

Abbreviations

SLE	systemic lupus erythematosus
2D-TEE	two-dimensional transesophageal echocardiography
3D-TEE	three-dimensional transesophageal echocardiography

TIA	transient ischemic attack
MRI	magnetic resonance imaging

REFERENCES

1. Libman E, Sacks B. A hitherto undescribed form of valvular and mural endocarditis. Arch Intern Med. 1924; 33:701–737.
2. Klemperer P, Pollack AD, Baehr G. Pathology of disseminated lupus erythematosus. Arch Pathol. 1941; 32:569–631.
3. Bridgen W, Bywaters EGL, Lessof MH, Ross IP. The heart in systemic lupus erythematosus. British Heart J. 1960; 22:1–16.
4. Bulkley BH, Roberts WC. The heart in systemic lupus erythematosus and the changes induced in it by corticosteroid therapy: a study of 36 necropsy patients. Am J Med. 1975; 58:243–264. [PubMed: 1115070]
5. Roldan CA, Shively BK, Crawford MH. An echocardiographic study of valvular heart disease associated with systemic lupus erythematosus. New Engl J Med. 1996; 335:1424–1430. [PubMed: 8875919]
6. Omdal R, Lunde P, Rasmussen K, Mellgren SI, Husby G. Transesophageal and transthoracic echocardiography and Doppler-examinations in systemic lupus erythematosus. Scand J Rheumatol. 2001; 30:275–281. [PubMed: 11727842]
7. Morelli S, Bernardo ML, Viganego F, Sgreccia A, De Marzio P, Conti F, et al. Left-sided heart valve abnormalities and risk of ischemic cerebrovascular accidents in patients with systemic lupus erythematosus. Lupus. 2003; 12:805–812. [PubMed: 14667095]
8. Roldan CA MD, Sibbitt WL Jr, Qualls CR, Jung RE, Greene ER, Gasparovic CM, et al. Libman-Sacks Endocarditis and Embolic Cerebrovascular Disease. JACC: Cardiovascular Imaging. 2013; 6:973–983. [PubMed: 24029368]
9. Avgoustidis N, Bourantas CV, Anastasiadis GP, Sipsas N, Pikazis D. Endocarditis due to Gemella haemolysans in a patient with systemic lupus erythematosus. J Heart Valve Dis. 2011; 20:107–109. [PubMed: 21404908]
10. Bouma W, Klinkenberg TJ, van der Horst IC, Wijdh-den Hamer IJ, Erasmus ME, Bijl M, et al. Mitral valve surgery for mitral regurgitation caused by Libman-Sacks endocarditis: a report of four cases and a systematic review of the literature. J Cardiothorac Surg. 2010; 5:13. [PubMed: 20331896]
11. Bernatsky S, Clarke A, Gladman DD, Urowitz M, Fortin PR, Barr SG, et al. Mortality related to cerebrovascular disease in systemic lupus erythematosus. Lupus. 2006; 15:835–839. [PubMed: 17211987]
12. Roldan CA, Qualls CR, Sopko KS, Sibbitt WL Jr. Transthoracic versus transesophageal echocardiography for detection of Libman-Sacks endocarditis: a randomized controlled study. J Rheumatol. 2008; 35:224–229. [PubMed: 18085739]
13. Zaragoza-Macias E, Chen MA, Gill EA. Real time three-dimensional echocardiography evaluation of intracardiac masses. Echocardiography. 2012; 29:207–219. [PubMed: 22283202]
14. Ahlgren B, Dorosz J, Rohrer A, Reece B, Cleveland J, Salcedo E, et al. Real time three-dimensional transesophageal echocardiography in the evaluation of two cases of rare mitral valve tumors. Echocardiography. 2012; 29:1011–1015. [PubMed: 22640169]
15. Liu YW, Tsai WC, Lin CC, Hsu CH, Li WT, Lin LJ, et al. Usefulness of real-time three-dimensional echocardiography for diagnosis of infective endocarditis. Scand Cardiovasc J. 2009; 43:318–323. [PubMed: 19199162]
16. Hansalia S, Biswas M, Dutta R, Hage FG, Hsiung MC, Nanda NC, et al. The value of live/real time three-dimensional transesophageal echocardiography in the assessment of valvular vegetations. Echocardiography. 2009; 26:1264–1273. [PubMed: 19929872]
17. Kampylafka EI, Alexopoulos H, Kosmidis ML, Panagiotakos DB, Vlachoyiannopoulos PG, Dalakas MC, et al. Incidence and prevalence of major central nervous system involvement in

systemic lupus erythematosus: a 3-year prospective study of 370 patients. PLoS One. 2013; 8:e55843. [PubMed: 23424638]

18. Sibbitt WL Jr, Schmidt PJ, Hart BL, Brooks WM. Fluid Attenuated Inversion Recovery (FLAIR) imaging in neuropsychiatric systemic lupus erythematosus. J Rheumatol. 2003; 30:1983–1989. [PubMed: 12966602]
19. Kozora E, Ellison MC, West S. Reliability and validity of the proposed American College of Rheumatology neuropsychological battery for systemic lupus erythematosus. Arthritis Rheum. 2004; 51:810–818. [PubMed: 15478145]
20. Hahn RT, Abraham T, Adams MS, Bruce CJ, Glas KE, Lang RM, et al. Guidelines for Performing a Comprehensive Transesophageal Echocardiographic Examination: Recommendations from the American Society of Echocardiography and the Society of Cardiovascular Anesthesiologists. J Am Soc Echocardiogr. 2013; 26:921–964. [PubMed: 23998692]
21. Lang RM, Badano LP, Tsang W, Adams DH, Agricola E, Buck T, et al. EAE/ASE Recommendations for Image Acquisition and Display Using Three-Dimensional Echocardiography. J Am Soc Echocardiogr. 2012; 25:3–46. [PubMed: 22183020]
22. Roldan CA, Shively BK, Crawford MH. Valve excrescences: prevalence, evolution and risk for cardioembolism. J Am Coll Cardiol. 1997; 30:1308–1314. [PubMed: 9350932]
23. Asch FM, Bieganski SP, Panza JA, Weissman NJ. Real-time 3-dimensional echocardiography evaluation of intracardiac masses. Echocardiography. 2006; 23:218–224. [PubMed: 16524392]
24. Plastiras SC, Pamboucas CA, Tektonidou M, Toumanidis ST. Real-time three-dimensional echocardiography in evaluating Libman-Sacks vegetations. Eur J Echocardiogr. 2010; 11:184–185. [PubMed: 19946116]
25. Plastiras SC, Pamboucas CA, Tzelepis GE, Toumanidis ST. Assessing mitral valve stenosis by real-time 3-dimensional echocardiography in systemic lupus erythematosus: a look inside the heart. J Rheumatol. 2009; 36:1843–1845. [PubMed: 19671828]
26. Shroff H, Benenstein R, Freedberg R, Mehl S, Saric M. Mitral valve Libman-Sacks endocarditis visualized by real time three-dimensional transesophageal echocardiography. Echocardiography. 2012; 29:E100–E101. [PubMed: 22176492]
27. Vatankulu MA, Erdogan E, Tasal A, Sonmez O, Cinar A, Aydin C, et al. The role of real time three-dimensional transesophageal echocardiography in assessing Libman-Sacks endocarditis. Echocardiography. 2012; 29:E216–E217. [PubMed: 22671937]
28. Unlü M, Demirkol S, Balta S, Küçük U. Mitral valve Libman-Sacks endocarditis evaluated by two and three-dimensional transesophageal echocardiography. Turk Kardiyol Dern Ars. 2013; 41:178. [PubMed: 23666313]
29. Buppajarntham S, Satitthummanid S, Chantranuwatana P, Luengtaviboon K, Chattranukulchai P, Boonyaratavej S, et al. Aortic valve papillary fibroelastoma associated with severe aortic regurgitation: a comprehensive assessment with 2- and 3-dimensional transesophageal echocardiography. J Am Coll Cardiol. 2012; 60:e41. [PubMed: 23217845]
30. Zoghbi WA, Enriquez-Sarano M, Foster E, Grayburn PA, Kraft CD, Levine RA, et al. Recommendations for evaluation of the severity of native valvular regurgitation with two-dimensional and Doppler echocardiography. J Am Soc Echocardiogr. 2003; 16:777–802. [PubMed: 12835667]
31. Lang RM, Tsang W, Weinert L, Mor-Avi V, Chandra S. Valvular Heart Disease : The Value of 3-Dimensional Echocardiography. J Am Coll Cardiol. 2011; 58:1933–1944. [PubMed: 22032703]
32. Hyodo E, Iwata S, Tugcu A, Arai K, Shimada K, Muro T, et al. Direct measurement of multiple vena contracta areas for assessing the severity of mitral regurgitation using 3D TEE. JACC Cardiovasc Imaging. 2012; 5:669–676. [PubMed: 22789934]
33. Schlosshan D, Aggarwal G, Mathur G, Allan R, Cranney G. Real-time 3D transesophageal echocardiography for the evaluation of rheumatic mitral stenosis. JACC Cardiovasc Imaging. 2011; 4:580–588. [PubMed: 21679891]

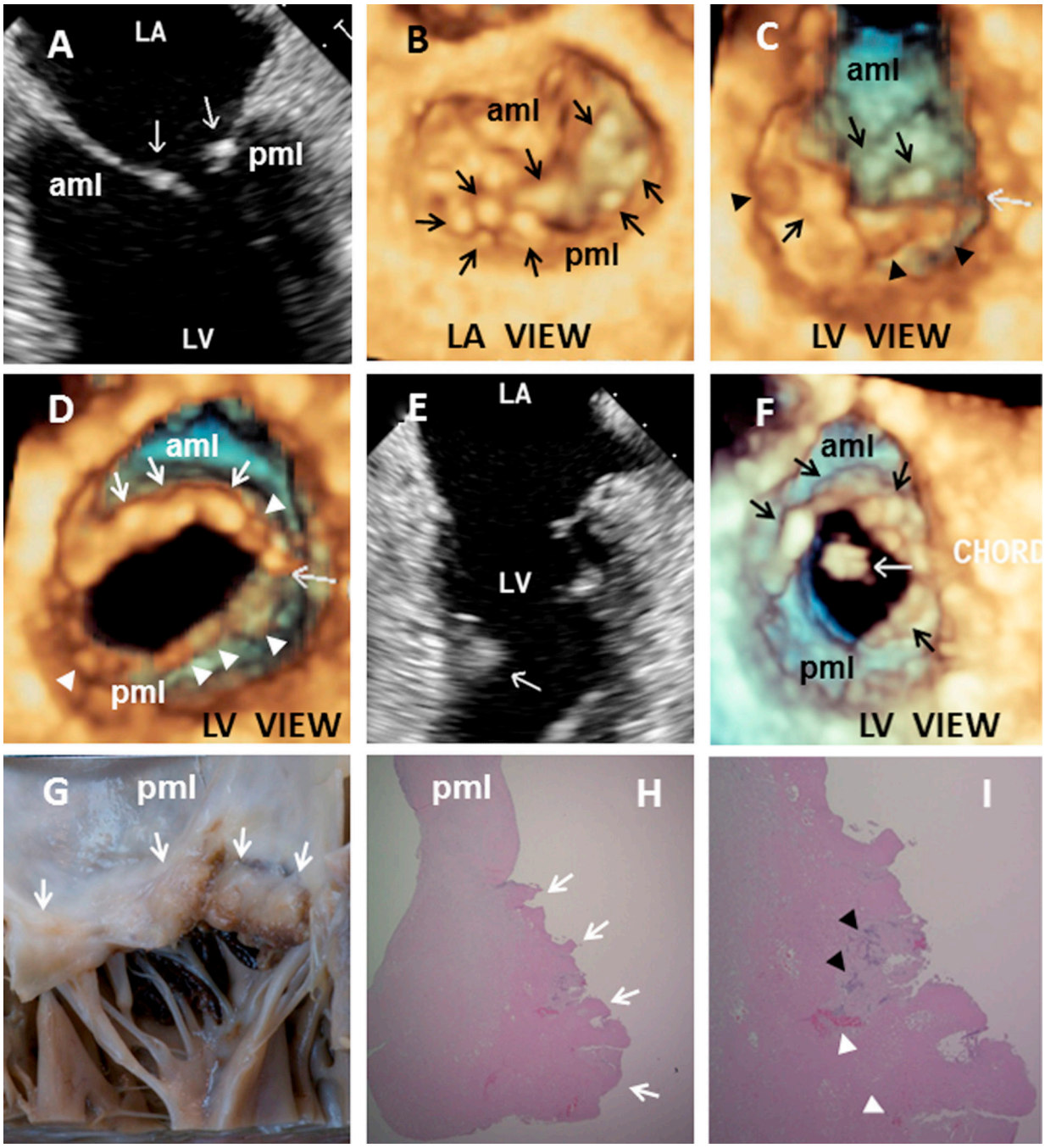

Figure 1. A 26 year old woman with SLE with past stroke and acute transient ischemic attack

A. This 2D-TEE four chamber view demonstrates small, irregular shape, sessile, and homogeneously hyperreflectant nodularities consistent with healed Libman-Sacks vegetations (*arrows*) on the left atrial (LA) side and distal portions of the anterior (aml) and posterior (pml) mitral leaflets associated with mild leaflets' thickening and severely decreased mobility of the posterior mitral leaflet (pml) (*see video clip 1A*). **B.** This 3D-TEE LA view of the mitral valve during systole demonstrates the additional findings of multiple, small to medium size, protruding, sessile, predominantly oval shape, and homogeneously

echoreflectant nodularities (*arrows*) involving all scallops and mostly but not exclusively located at the tip of both leaflets (*see video clip 1B*); **C.** This 3D-TEE left ventricular (LV) view of the mitral valve during systole also demonstrates 1) multiple, small to medium size, protruding, and homogeneously echoreflectant nodularities (*arrows*) located mainly at the tip of the anterior and posterior mitral leaflets; and 2) three small to medium size, oval and tubular shape, sessile, and with brown discoloration vegetations located on the tip and commissural portion of P3, tip of P2, and tip of P1 scallops (*arrowheads*) suggestive of recently formed vegetations (*see video clip 1C*). **D.** This 3D-TEE LV view of the mitral valve during diastole demonstrates 1) multiple nodularities with homogeneous (arrows) and heterogeneous (arrowheads) echoreflectance along the tip of both mitral leaflets (*arrows*), 2) decreased mobility of both leaflets, of severe degree for the posterior leaftet with fixed P1 and P2 scallops, and 3) mild degree of anterolateral commissural fusion (*horizontal arrow*) (*see video clip 1C*). **E.** This 2D-TEE two-chamber view demonstrates a large oval and homogeneously soft tissue echoreflectant mass suggestive of a recently formed vegetation (arrow) located at the junction of the posteromedial papillary muscle tip and chorda tendinae (*see video clip 1E*). **F.** This 3D-TEE LV view of the subvalvular mitral valve apparatus demonstrates a medium size chordal vegetation *(horizontal arrow*) in addition to multiple nodularities (probably healed vegetations) on the tip portion of both mitral leaflets (*see video clip 1F*). Associated moderate mitral regurgitation was demonstrated by color Doppler. **G.** This photograph of the middle scallop of the posterior mitral leaflet (pml) demonstrates sessile, granular, protruding, grayish to brown discoloration, clustered, and coalescent Libman-Sacks vegetations (arrows) located on the coaptation point and predominantly on the atrial side, but also extending to the ventricular side of the leaflet. **H.** This H&E histopathologic section at low magnification (2×) of the posterior mitral leaflet (pml) demonstrates diffuse thickening predominant of the leaflet tip with a well adhered vegetation mainly on the atrial side, but also extending to the ventricular side (arrows). Note that the demarcation between the vegetation and leaflet is poorly defined. **I**. This H&E histopathologic section of the Libman-Sacks vegetation at higher magnification (4×) demonstrated areas of fibrinoid necrosis (black arrowhead), focal hemorrhages (white arrowhead), few scattered acute inflammatory infiltrates, and interspersed fibrinous thrombi deposition (pink color tissue). Of note, the patient's brain histopathology also confirmed multiple micro and macroinfarcts in different stages and a thrombotic vasculopathy.

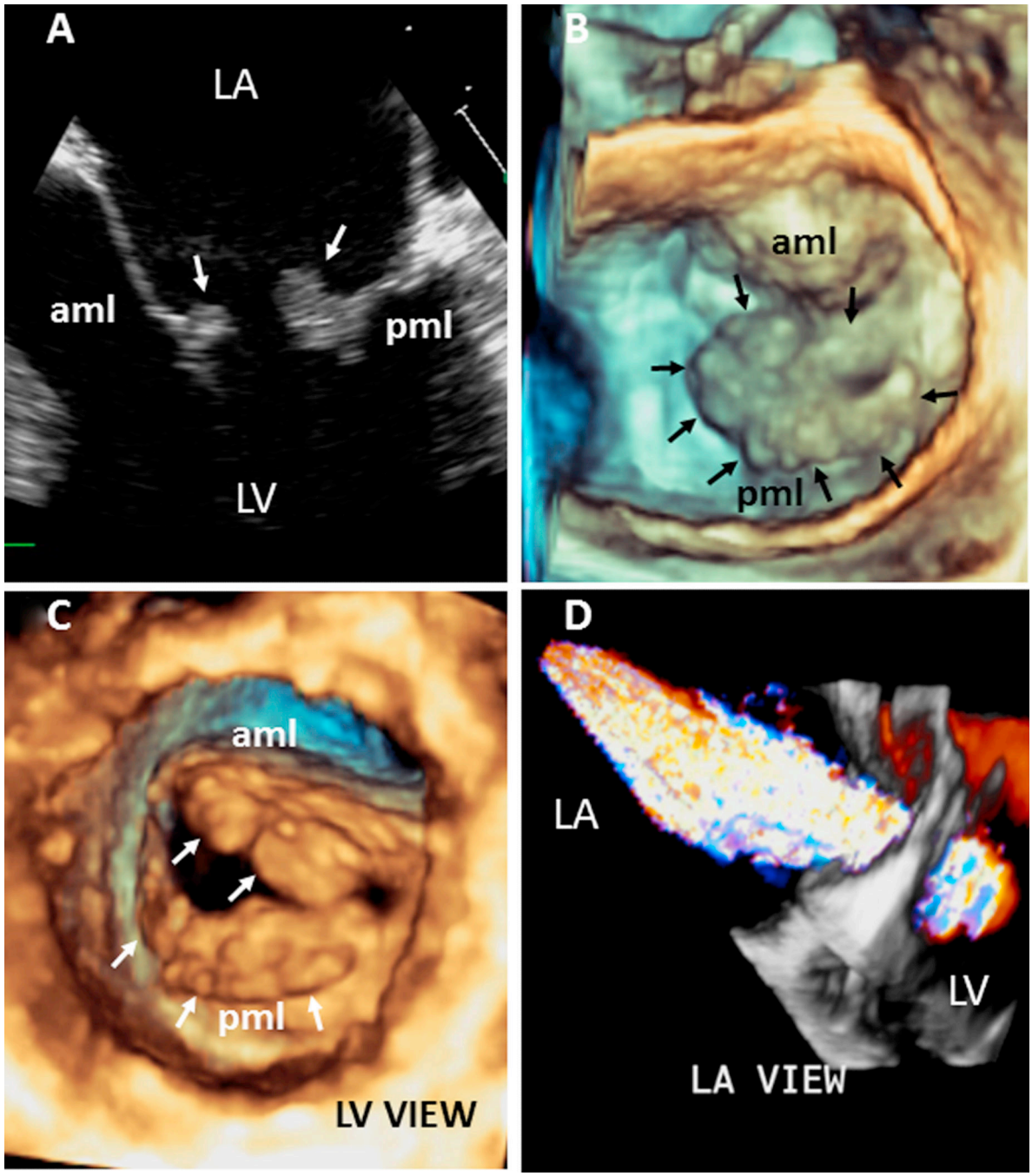

Figure 2. A 29 year old male with SLE and acute stroke

A. This 2-D TEE four chamber close-up view of the mitral valve demonstrates medium to large size, oval shape, sessile, and homogeneously soft tissue echoreflectant Libman-Sacks vegetations on the atrial side and distal portions of the anterior (aml) and posterior (pml) mitral leaflets (*arrows*) associated with mild leaflets' tip thickening and decreased mobility (*see video clip 2A*). **B,C.** This 3D-TEE LA view during systole (**B**) and LV view during diastole (**C**) of the mitral valve demonstrate the additional findings of large, severely protruding, with irregular surface, tubular and multilobed shape, and with roll-like motion

(move from atrial to ventricular side during diastole) vegetations located on the atrial side and tip of the entire anterior (aml) and posterior (pml) mitral leaflets (*arrows*) with associated decreased mobility and incomplete coaptation of the leaflets (*see video clips 2B, 2C)*. Associated severe mitral regurgitation was demonstrated by color-Doppler (*see video clip 2D*).

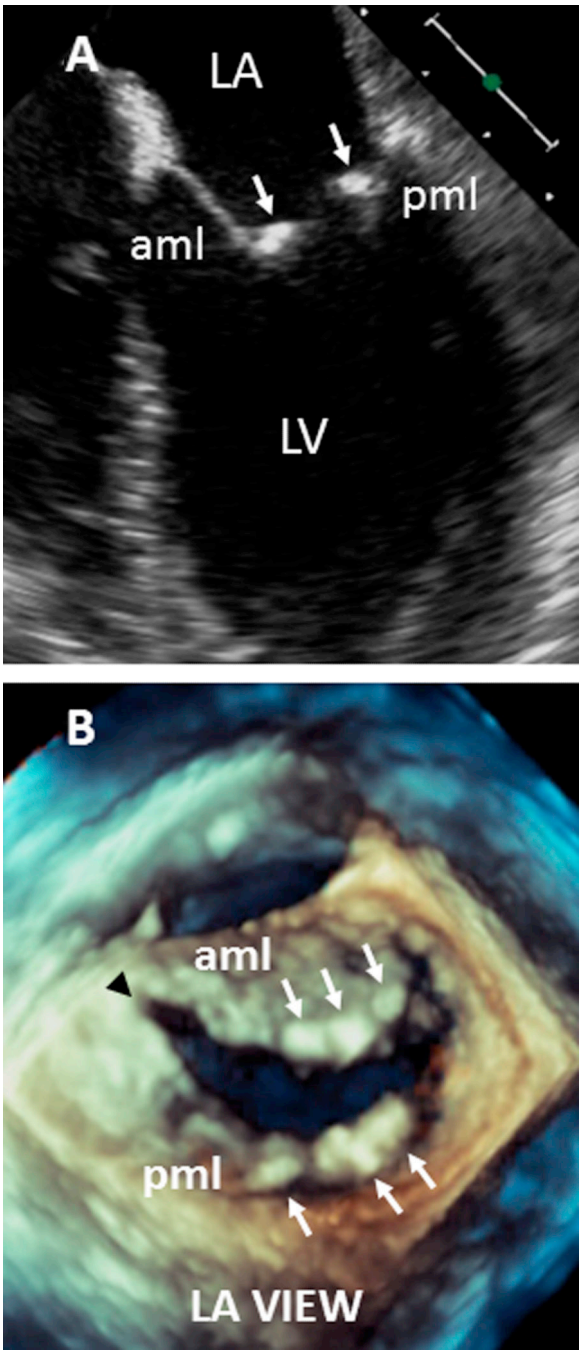

Figure 3. A 50 year old woman with SLE, past stroke, and acute transient ischemic attack

A. This 2D-TEE four chamber view demonstrates small to medium size, irregular shape, sessile, and homogeneously hyperreflectant nodularities located on the atrial side and tip of the anterior (aml) and posterior (pml) mitral leaflets (*see video clip 3A*). These findings are consistent with healed Libman-Sacks vegetations. **B**. This 3D-TEE LA view of the mitral valve demonstrates multiple, contiguous, protruding, and homogeneously hyperreflectant nodularities consistent with healed vegetations (*arrows*) located on the atrial side and leaflet tips of the middle and posteromedial scallops of the anterior (aml) and posterior (pml) mitral

leaflets (*see video clip 3B*). Associated decreased mobility predominantly of the posterior mitral leaflet and mild anterolateral commissural fusion (*arrowhead*) is noted. Moderate mitral regurgitation was demonstrated by color Doppler.

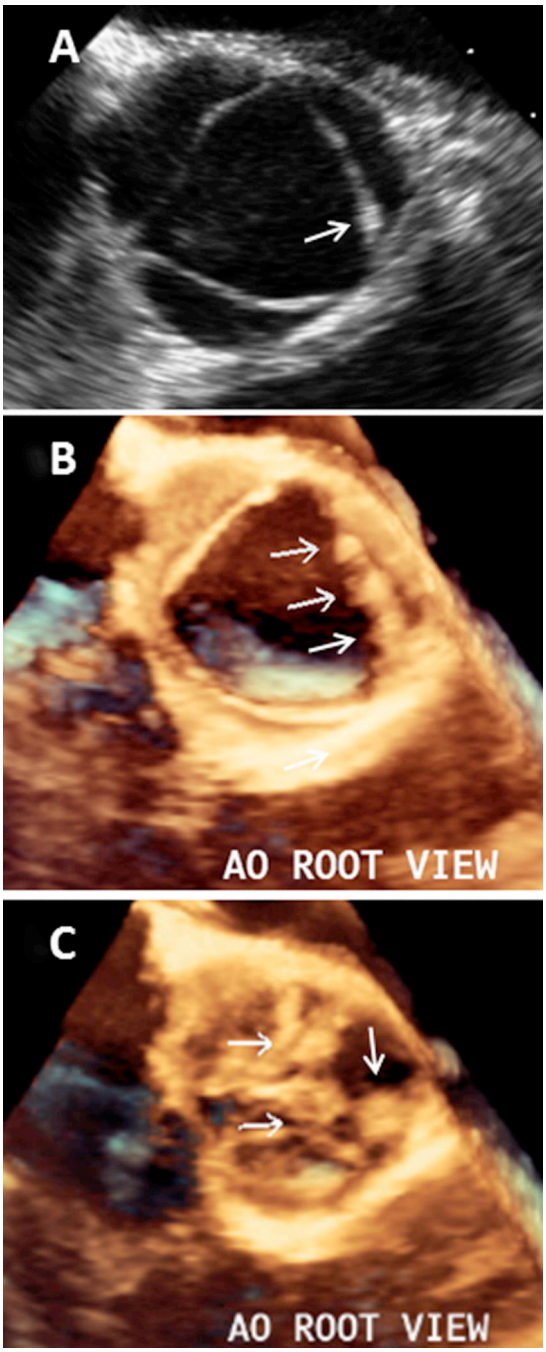

Figure 4. A 29 year old male with SLE and recurrent TIA

A. This 2D-TEE short axis view of the aortic valve demonstrates a small focal area of mild thickening of the tip of the left coronary cusp (*arrow*) (*see video clip 4A*). **B.** This 3D-TEE aortic root view of the aortic valve during systole demonstrates 3 contiguous, oval shape, small size, sessile, with irregular borders, and homogeneously echoreflectant vegetations on the aortic side and tip of the left coronary cusp (*arrows*) (*see video clip 4B*). **C.** This 3D-TEE aortic root view of the aortic valve during diastole defines better the characteristics and

location of the 3 vegetations (*arrows*) (*see video clip 4B*). Associated mild aortic regurgitation was demonstrated by color Doppler.

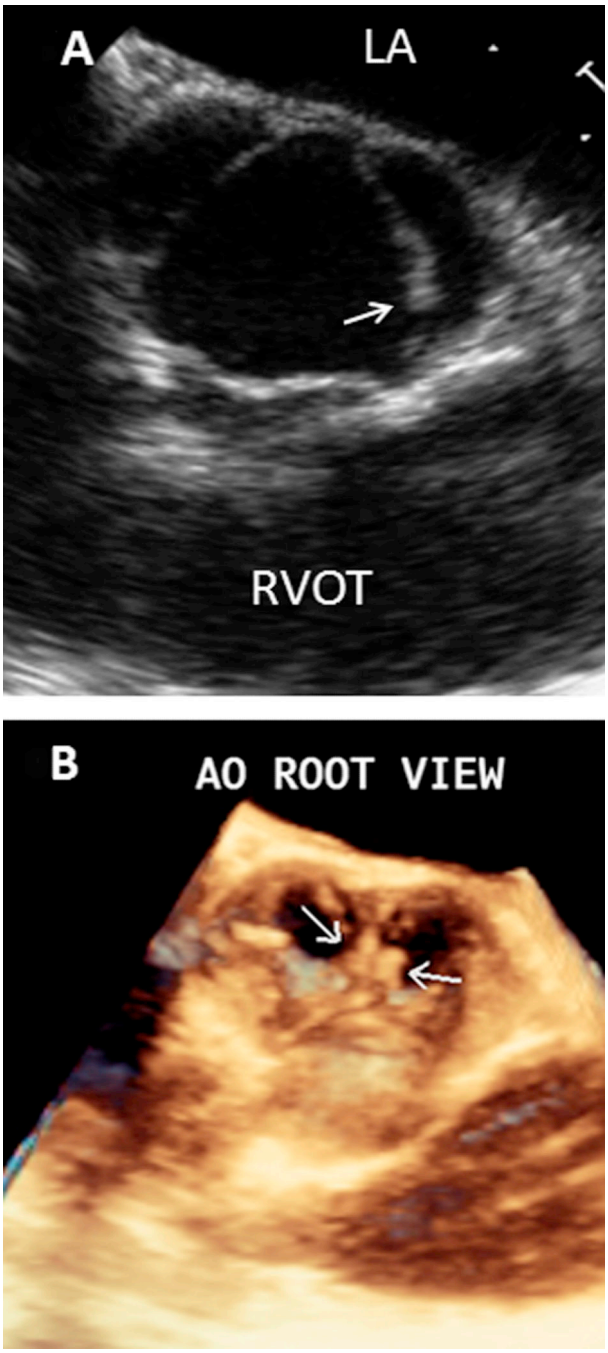

Figure 5. A 38 year old woman with a recent transient ischemic attack

A. This 2D-TEE short axis view of the aortic valve demonstrates mild focal thickening of the tip of the left coronary cusp (*arrow*) (see *video clip 5A*). The appearance of the non-coronary and right coronary cusps is unremarkable. **B.** This 3D-TEE aortic root view of the aortic valve demonstrates 2 small, irregular shape, and sessile vegetations on the aortic side and tip portions of the non-coronary and left coronary cusps (*arrows*) (*see video clip 5B*). No aortic regurgitation was demonstrated by color Doppler.

Table 1

Clinical, Laboratory, and Therapy Data in Patients with SLE

Characteristic	Patients (N = 29)
Duration of SLE (years)	6.2 ± 5.6
Age at diagnosis of SLE (years)	27.5 ± 11.1
Total SLEDAI (U)	12.6 ± 11.8
Total SLICC (U)	2.8 ± 1.8
White blood cells count (cell count per cm^3)	6.9 ± 2.9
Hemoglobin (mg/dL)	12.9 ± 2.0
Platelets (counts per cm^3)	243.6 ± 76.7
Creatinine (mg/dL)	1.33 ± 1.81
Serum albumin (mg/dL)	3.6 ± 0.6
dsDNA titer	247.3 ± 540.1
ANA titer	895.8 ± 818.0
C3 (mg/dl)	93.1 ± 39.8
C4 (mg/dl)	14.8 ± 8.8
CH50 (mg/dl)	69.1 ± 44.1
Quantitative D-dimer (mg/dL)	0.95 ± 1.2
C-reactive protein (mg/dl)	1.3 ± 1.2
Erythrosedimentation rate (mm/hr)	40.5 ± 23.8
Smith antibody positive	14 (48%)
SSA antibody positive	12 (41%)
SSB antibody positive	9 (31%)
Any antiphospholipid antibody positive	16 (58%)
Beta-2 glycoprotein I antibody positive	8 (28%)
Lupus-like inhibitor positive	10 (34%)
IgG, IgM, or IgA anticardiolipin positive	14 (48%)
Prednisone therapy	16 (55%)
Prednisone current dose (mg/d)	21.0 ± 44
Prednisone average dose (mg/day)	5.4 ± 4.5
Years of prednisone	4.8 ± 4.6
Cyclophosphamide therapy	10 (34%)
Any immunosuppressive therapy (beyond prednisone)	12 (41%)
Hydroxycloroquine or cloroquine therapy	20 (69%)
Aspirin, clopidogrel, or warfarin	11 (38%)

Cell formats are mean ± SD or frequency (%).

Abbreviations: SLE = systemic lupus erythematosus, SLEDAI = SLE disease activity index, SLICC = Systemic Lupus International Collaborating Clinics, DNA = double stranded nuclear antibody, ANA = antinuclear antibody, SSA = Ro antibody, SSB = La antibody.

Table 2

Detection and Characterization of Libman-Sacks Vegetations by 3D-TEE and 2D-TEE

Valve	3D-TEE N = 40	2D-TEE N = 40	P value
TEE Studies with Vegetations			
Mitral valve	18 (45%)	14 (35%)	0.046*
Aortic valve	19 (48%)	12 (30%)	0.008*
Either valve	26 (65%)	20 (50%)	0.01*
Number of Vegetations			
Mitral valve	59 (1.48)	42 (1.05)	0.09†
Aortic valve	31 (0.78)	15 (0.38)	<0.001†
Either valve	90 (2.25)	57 (1.43)	0.001†
Maximum Diameter and Area of Vegetations			
Mitral valve vegetations (diameter, mm)	9.16 ± 5.76	5.3 ± 4.15	0.03‡
Mitral valve vegetations (area, cm^2)	0.58 ± 0.46	0.26 ± 0.34	0.049‡
Aortic valve vegetations (diameter, mm)	5.59 ± 1.61	3.9 ± 1.26	0.005‡
Aortic valve vegetations (area, cm^2)	0.15 ± 0.07	0.12 ± 0.08	0.21‡

*Paired comparisons by McNemar's test in this section; format is number of studies with vegetations (%)

†Paired comparisons are by Poisson regression in this section; format is number of vegetations (mean number of vegetations per study)

‡Paired comparisons are by paired t-test in this section; format is mean diameter or area ± SD

Table 3

Location of Libman-Sacks Vegetations by 3D-TEE and 2D-TEE

	3D-TEE N=40	2D-TEE N=40	P value*
Mitral Valve			
Anterior leaflet	35 (0.88)	19 (0.48)	0.02
Posterior leaflet	21 (0.53)	19 (0.48)	0.68
Distal portion of anterior or posterior leaflets	41 (1.03)	34 (0.85)	0.26
Mid or proximal portion of mitral leaflets	15 (0.38)	4 (0.10)	0.07
Middle (A2 or P2) scallops	30 (0.75)	26 (0.65)	0.46
Anterolateral (A1,P1) or posteromedial (A3,P3) scallops	26 (0.65)	12 (0.30)	0.046
Ventricular side	9 (0.23)	6 (0.15)	0.07
Atrial to ventricular side (protruding through leafelt)	4 (0.10)	2 (0.05)	0.14
Left ventricular or both atrial and ventricular side	11 (0.28)	6 (0.15)	0.04
Vegetations involving 2 or 3 contiguous scallops	15 (0.38)	7 (0.18)	0.03
Aortic Valve			
Right coronary cusp	8 (0.20)	7 (0.18)	0.55
Left coronary cusp	9 (0.23)	3 (0.08)	0.05
Non-coronary cusp	14 (0.35)	5 (0.13)	0.002
Coronary cusps tip	18 (0.45)	8 (0.20)	0.009
Coronary cusps body	3 (0.08)	5 (0.13)	0.46
Coronary cusps margin	10 (0.25)	2 (0.05)	0.004
Ventricular side	6 (0.15)	6 (0.15)	1.0
Aortic side	6 (15%)	2 (5%)	0.14
Ventricular to aortic side (protruding trough)	11 (28%)	1 (3%)	0.02
Both aortic or aortic and ventricular side	16 (40%)	3 (8%)	0.01

*All p values by Poisson regression; format is number of vegetations (mean number of vegetations per study).

Table 4

Detection of Associated Commissural Fusion by 3D-TEE and 2D-TEE

	3D-TEE N = 40	2D-TEE N = 40	P value
Mitral Valve			
Anterolateral commissure	5 (13%)	2 (5%)	0.08
Posteromedial commissure	6 (15%)	1 (3%)	0.03
Either commissure	8 (20%)	2 (5%)	0.01
Aortic Valve			
Non-coronary - left coronary cusps commissure	1 (3%)	0	1.0
Non-coronary - right coronary cusps commissure	2 (5%)	0	0.50
Right coronary - left coronary cusps commissure	3 (8%)	0	0.50
Any commissure	4 (10%)	0	0.08
Either Mitral or Aortic Valve			
Any mitral or aortic valve commissure	12 (30%)	2 (5%)	0.002

Table 5

Detection of Libman-Sacks Vegetations by 3D-TEE and 2D-TEE in Patients with Acute Neurologic Syndromes, Focal Brain Injury on MRI, Cognitive Dysfunction, or Any Cerebrovascular Disease

Outcome	Patients with vegetations on 3D-TEE	Patients with vegetations on 2D-TEE	P value*
Patients with acute neurologic syndromes (n = 23)	18 (78%)	15 (65%)	0.08
Patients with acute stroke/TIA (n = 18)	16 (89%)	13 (72%)	0.08
Patients with focal brain injury on MRI (n = 25)	20 (80%)	16 (64%)	0.045
Patients with neurocognitive dysfunction (n = 27)	19 (70%)	15 (56%)	0.046
†Patients with any cerebrovascular disease (n = 34)	24 (71%)	18 (53%)	0.01

*By McNemar's test for paired comparisons of vegetations by 3D-TEE and 2D-TEE.

†As noted in the Table, many patients had more than one type of cerebrovascular disease.

Cerebrovascular disease = acute neurologic syndromes, focal brain injury on MRI, or neurocognitive dysfunction.